Investigation of the Anomalous Spectroscopic Features of the Copper Sites in Chicken Ceruloplasmin: Comparison to Human Ceruloplasmin†

Timothy E. Machonkin,‡ Giovanni Musci,§ Hua H. Zhang,‡ Maria Carmela Bonaccorsi di Patti,|| Lilia Calabrese,⊥ Britt Hedman,▽ Keith O. Hodgson,‡,▽ and Edward I. Solomon*,‡

Department of Chemistry and Stanford Synchrotron Radiation Laboratory, Stanford University, Stanford, California 94305, Department of Organic and Biological Chemistry, University of Messina, Salita Sperone, 31, 98166 Messina, Italy, Department of Biochemical Sciences, University La Sapienza, Piazzale Aldo Moro 5, 00185, Rome Italy, and Department of Biology, University Roma Tre, viale Marconi 446, 00146, Rome, Italy

Received February 5, 1999; Revised Manuscript Received April 27, 1999

ABSTRACT: Chicken ceruloplasmin has been previously reported to display a number of key differences relative to human ceruloplasmin: a lower copper content and a lack of a type 2 copper signal by electron paramagnetic resonance (EPR) spectroscopy. We have studied the copper sites of chicken ceruloplasmin in order to probe the origin of these differences, focusing on two forms of the enzyme: "resting" (as isolated by a fast, one-step procedure) and "peroxide-oxidized". From X-ray absorption, EPR, and UV/visible absorption spectroscopies, we have shown that all of the copper sites are oxidized in peroxide-oxidized chicken ceruloplasmin and that none of the type 1 copper sites display the EPR features typical for type 1 copper sites that lack an axial methionine. In the resting form, the type 2 copper center is reduced. Upon oxidation, it does not appear in the EPR spectrum at 77 K, but it can be observed by using magnetic susceptibility, EPR at ∼8 K, and magnetic circular dichroism spectroscopy. It displays unusually fast relaxation, indicative of coupling with the adjacent type 3 copper pair of the trinuclear copper cluster. From reductive titrations, we have found that the reduction potential of the type 2 center is higher than those of the other copper sites, thus explaining why it is reduced in the resting form. These results provide new insight into the nature of the additional type 1 copper sites and the redox distribution among copper sites in the different ceruloplasmins relative to other multicopper oxidases.

The multicopper oxidases are a broad class of enzymes that couple the four-electron reduction of dioxygen to water with four sequential one-electron oxidations of substrate via a ping-pong mechanism (*1*). This class of enzymes includes the plant and fungal laccases, ascorbate oxidase, ceruloplasmin, and other recently characterized enzymes such as Fet3 protein (the protein encoded by the *FET3* gene, one of the genes involved in the high-affinity iron transport system of *Saccharomyces cerevisiae*) (*2*−*4*) and phenoxazinone synthase (*5*−*7*). They contain copper ions of the following types: at least one blue copper or type 1 site (T1)[1] characterized by an absorption band of ∼5000 M^{-1} cm^{-1} at ∼600 nm and narrow parallel hyperfine splitting [$A_{||} = (43-95) \times 10^{-4}$ cm^{-1}] in the electron paramagnetic resonance (EPR) spectrum, a normal or type 2 site (T2) characterized by the lack of intense absorption bands and normal EPR features [$A_{||} = (158-201) \times 10^{-4}$ cm^{-1}], and a type 3 copper pair (T3) characterized by an absorption band of ∼5000 M^{-1} cm^{-1} at ∼330 nm and strong antiferromagnetic coupling leading to the lack of an EPR signal. The T2 and T3 sites form a trinuclear cluster, which is the site for dioxygen reduction (*8*−*11*), while the function of the T1 site is to transfer electrons from substrate to the trinuclear cluster and thus is the site for substrate oxidation.

The copper sites of *Rhus vernicifera* laccase have been extensively spectroscopically characterized. These data, together with crystal structures of ascorbate oxidase in both the oxidized (*11*) and reduced (*12*) forms and of a T2-depleted form of a fungal laccase (*13*), provide a great deal of mechanistic insight into how the trinuclear copper cluster functions to reduce dioxygen to water and how electrons are transferred from substrate to the T1 site and then to the trinuclear cluster. In contrast to the other multicopper oxidases, ceruloplasmin (Cp) is unique in that it contains additional copper sites beyond the four required for oxidase

† This research was supported by NIH Grant DK31450 to E.I.S. and NIH Grant CHE-9423181 to K.O.H. SSRL is supported by the Department of Energy, Office of Basic Energy Sciences, Division of Chemical and Material Science, and in part by the NIH, National Center for Research Resources, Biomedical Technology Program, and by DOE's Office of Biological and Environmental Research. T.E.M. was supported by an NSF predoctoral fellowship and a Stanford University Leibermann Fellowship.

* To whom correspondence should be addressed: Phone or fax (650) 723-9104; Email solomon@chem.stanford.edu.

‡ Department of Chemistry, Stanford University.

§ Department of Organic and Biological Chemistry, University of Messina.

|| Department of Biochemical Sciences, University La Sapienza.

⊥ Department of Biology, University Roma Tre.

▽ Stanford Synchrotron Radiation Laboratory, Stanford University.

[1] Abbreviations: BSA, bovine serum albumin; Cp, ceruloplasmin; EPR, electron paramagnetic resonance; MCD, magnetic circular dichroism; MES, 2-(*N*-morpholino)ethanesulfonic acid; 1,2-MeIm, 1,2-dimethylimidazole; MePY2, methylbis(2-pyridylethyl)amine; MOPS, 2-(*N*-morpholino)propanesulfonic acid; NHE, normal hydrogen electrode; SDS−PAGE, sodium dodecyl sulfate−polyacrylamide gel electrophoresis; SQUID, superconducting quantum interference device; T1, type 1; T1Hg, mercury-substituted type 1 derivative; T1PR, type 1 permanently reduced; T2, type 2; T3, type 3; XAS, X-ray absorption spectroscopy.

10.1021/bi990280z CCC: $18.00
Published on Web 08/05/1999

activity. Human Cp contains six integral copper sites per molecule, with an additional labile copper-binding site that does not alter the oxidase activity, as early reported by Huber and Frieden (*14*). The crystal structure of Zaitseva et al. (*15*) confirmed a stoichiometry of six copper sites: a trinuclear cluster and three coppers bound to the three T1-binding sites. Early spectroscopic studies of human Cp appeared to be inconsistent with this copper stoichiometry (*16*−*22*). We recently reexamined the copper sites in human Cp using X-ray absorption spectroscopy (XAS), SQUID magnetic susceptibility, and EPR and determined that one of the T1 copper sites, likely the one in domain two that lacks an axial methionine, stays reduced and is functionally inactive due to a high reduction potential (*23*).

Recently, a rapid one-step procedure was used to purify a Cp from chicken that displayed a number of key differences relative to human Cp (*24*): the copper content was 5.01 ± 0.35, based upon a molecular mass of 140 kDa determined by SDS−PAGE [compared with 132 kDa for human Cp, as first accurately determined by low-resolution X-ray crystallography (*25*)], and the EPR spectrum lacked any detectable low-field hyperfine line of a T2 copper and integrated to 50% of the total copper content. Despite these differences, purified chicken Cp still retained oxidase activity and, in fact, was about 5 times *more* active than human Cp at the same pH. On the basis of the copper content and EPR features, it was proposed that chicken Cp contained two T1 copper sites and a T2/T3 trinuclear cluster that exhibited unusual magnetic coupling such that it lacked resolvable hyperfine and quantitated to 0.5 copper by EPR double integration. Furthermore, upon reduction and reoxidation, all of the T1 copper features reappeared quickly, in contrast to what has been previously reported for human Cp, in which, in the absence of adventitious iron, 50% of the T1 copper reappears within 20 ms and the other 50% does not reappear for >20 h (*26*, *27*). In our previous study of human Cp, we found that the apparent discrepancy between the crystallographic results and the earlier spectroscopic results was because of the presence of reduced copper. In human Cp isolated by the rapid one-step method (*20*), two of the six copper ions are reduced: one reducing equivalent is associated with the reduced, redox-inactive T1 copper, while the other is distributed among the redox-active T1, T2, and T3 copper sites in an approximate ratio of 0.5:0.3:0.2; this latter equivalent could be oxidized by H_2O_2. We have performed a parallel study on chicken Cp, again focusing on two different forms of the enzyme, a "resting" form, which is the enzyme as isolated by the rapid one-step method, and a "peroxide-oxidized" form, which is the resting form treated with a 20−30-fold excess of H_2O_2 for 1−3 h.[2] We have used copper K-edge X-ray absorption spectroscopy (XAS), absorption, and EPR at liquid nitrogen temperature to quantitate the amount of reduced copper and determine its distribution, and we have used Curie slope SQUID magnetic susceptibility, EPR at liquid helium temperature, and magnetic circular dichroism (MCD) spectroscopy to probe the coupling in the trinuclear cluster.

[2] Some samples were additionally reacted with a 50-fold excess of $[Fe(CN)_6]^{3-}$; these samples showed no differences as compared to those oxidized with H_2O_2 alone.

EXPERIMENTAL PROCEDURES

The chloroethylamine used in the derivatization of Sepharose 4B was recrystallized from hot ethanol. Water was purified to a resistivity of 15.5−17 MΩ cm^{-1} by use of a Barnstead Nanopure deionization system. $[Cu(1,2\text{-MeIm})_2](PF_6)$ and $[(MePy_2)Cu(CH_3CN)](ClO_4)$ were kindly provided by Professor Ken Karlin at Johns Hopkins University. All other chemicals used were reagent-grade and were used without further purification.

Chicken Cp was purified by the rapid one-step method (*20*, *24*), and some of it was repurified by a modification of this procedure (*23*). The 610/280 ratio of resting purified Cp was about 0.060. All samples were kept frozen at −80 °C until use. Protein concentration was determined by the microbiuret assay (*28*). Total copper concentration was determined by the biquinoline assay (*29*), with protein aliquots containing 170−425 μM copper and referenced with a blank containing the buffer. The copper content of the buffers were determined by use of a Perkin-Elmer 2380 atomic absorption (AA) spectrometer with a HGA-400 graphite furnace: phosphate buffer contained 1.1 μM copper, and MES buffer contained 0.60 μM copper. Copper content determined by the biquinoline assay was checked with the graphite furnace AA and found to be consistent. Average total copper content (from eight separate batches of protein) was 5.65 ± 0.23 coppers per molecule.

Peroxide-oxidized Cp was prepared by incubation of resting Cp with a 20−30-fold excess of H_2O_2 for 1−3 h at 4 °C. This was removed from some of the samples by passage through a G-25 column; the samples were then reconcentrated by using Centricon concentrators. The oxidant was always removed in samples used for the SQUID susceptibility measurements or reductive titration experiments. A few samples (for example, the Q-band EPR samples and some of the XAS samples) also contained a 50-fold excess of $[Fe(CN)_6]^{3-}$; these samples showed no differences as compared to those oxidized with H_2O_2 alone. Protein concentrations were in the range of 0.02−0.10 mM for most absorption and EPR measurements; for XAS, SQUID, Q-band EPR, and MCD experiments, protein concentrations were typically 0.1−1.0 mM. All samples for all experiments were run in 0.2 M potassium phosphate buffer, pH 7.0, except for samples prepared for SQUID susceptibility. Since potassium phosphate buffer contains unacceptable levels of ferric impurities, Cp samples for SQUID susceptibility were exchanged into deuterated 0.1 M MOPS buffer, pD 7.0. Cp samples in MOPS buffer showed no differences from those in phosphate buffer, except for slight differences in the EPR line widths.

Absorption spectra were recorded on a Hewlett-Packard HP8452A diode array spectrophotometer in a 1-cm path length cuvette. X- and Q-band EPR spectra were obtained with a Bruker ER 220-D-SRC spectrometer. For X-band EPR, sample temperatures were maintained at 77 K with a liquid nitrogen finger dewar or at ∼8 K with an Air Products Helitran LTR. For Q-band EPR, sample temperatures were maintained at 98 K with a nitrogen flow system. EPR spectra were spin-quantitated by comparison with a 1.0 mM aqueous copper standard run in the same tube as the sample where possible (*30*). EPR spectra were simulated by use of SIM15, obtained from the Quantum Chemistry Program Exchange

and modified to allow for anisotropic line widths. MCD spectra were obtained in the UV−visible region with a Jasco J-500-C spectropolarimeter, operating with an S-20 photomultiplier tube, and in the near-IR region with a Jasco J-200-D spectropolarimeter and a liquid nitrogen-cooled InSb detector. MCD spectra were obtained by use of a sample cell consisting of two quartz disks with a 3 mm rubber spacer. All protein samples contained approximately 60 vol % glycerol, to form an optical-quality glass upon freezing. The data were corrected for zero-field baseline effects induced by cracks in the glass by subtracting the corresponding 0 T scan.

XAS data were measured at the Stanford Synchrotron Radiation Laboratory on unfocused 8-pole wiggler beamline 7-3 under dedicated conditions (3.0 GeV, 60−100 mA). Monochromatic radiation was obtained from a Si(220) double-crystal monochromator, which was detuned 50% for harmonic rejection. The beam height was defined to be 1 mm. The fluorescence signals were measured with an argon-filled ionization chamber detector equipped with Soller slits and a Ni filter (*31*, *32*). Internal energy calibration was performed by simultaneous measurement of the absorption of a copper foil placed between the second and third ionization chambers. The first inflection point of the copper foil spectrum was assigned to 8980.3 eV. The samples were loaded into 2 mm Lucite XAS cells with 63.5 μm Mylar windows, frozen immediately, and kept under liquid nitrogen prior to measurements. The samples were maintained at a constant temperature of 10 K throughout the measurements by an Oxford Instruments CF1208 continuous-flow liquid helium cryostat. The data represent an average of four scans for each Cp sample.

Magnetic susceptibility data were taken on a Quantum Design model MPMS SQUID magnetometer. A palladium standard was used as a calibrant. Protein samples were loaded in polycarbonate capsules sealed with a drop of acetone and with a small hole in the top in order to flush the space above the sample. These were then loaded into a plastic drinking straw attached to the end of the magnetometer drive rod. Samples were evacuated and flushed with helium gas and then loaded into the probe maintained at 10 K. After loading, the samples were heated to 125 K and maintained at that temperature for 10 min to removed any condensed oxygen. Susceptibility data were collected versus $1/T$ in the temperature range of 5.25−115 K and at a field of 3.5 T. Sample volumes were 150 μL. To account for trace metal impurities and other extraneous paramagnetic signals, a blank sample of either buffer or bovine serum albumin (BSA) at the same mg mL^{-1} concentration in the same buffer was run and subtracted from the data. All samples were degassed by pump-purging at ~0 °C under argon.

Relative reduction potentials of the copper sites were determined by the reductive titration method (*33*). A ~50 μM solution of chicken Cp in 0.2 M potassium phosphate buffer at pH 7.0 was degassed by pump-purging at 0 °C under argon and brought into an anaerobic wet box. A stock solution of reductant, $Fe(NH_4)_2(SO_4)_2 \cdot 6H_2O$, was prepared in the box with water that was previously degassed by multiple freeze−pump−thaw cycles. Both the protein solution and the reductant solution were kept cold until use. A 200 μL aliquot of the protein solution was mixed with 1 electron equiv (assuming 6 coppers per protein molecule) of reductant solution and transferred to a 1 cm path length anaerobic cuvette with a Teflon stopcock. Absorption spectra were taken at room temperature after allowing sufficient time for complete reaction (generally about 15 min). This procedure was then repeated with a fresh 200 μL aliquot of protein and 2 electron equiv of reductant solution, then again for 3 electron equiv, and so on up to 7 electron equiv. Simulations of the reductive titration data were performed with Excel (Microsoft) and Mathcad (Mathsoft).

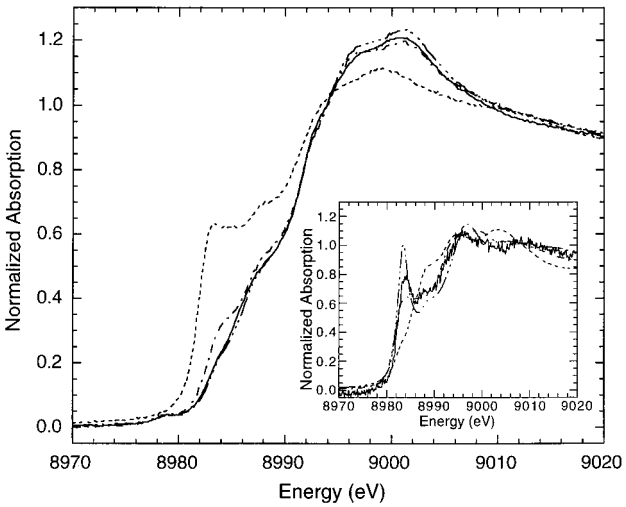

FIGURE 1: Normalized copper K-edge XAS of the fully oxidized model spectrum (—), peroxide-oxidized chicken Cp (—···—), resting chicken Cp (—·—) and reduced chicken Cp (- - -). Inset: Renormalized XAS of the reduced T2 copper site generated by subtraction of the oxidized T1Hg laccase XAS and two oxidized plastocyanin edges from the peroxide-oxidized chicken Cp XAS (—); the normalized XAS of known two-coordinate ($[Cu(1,2\text{-}MeIm)_2]PF_6$) (—···—), three-coordinate [T1Hg laccase (*4*)] (—·—), and four-coordinate Cu(I) ($[(MePY2)Cu(CH_3CN)]ClO_4$) (- - -) sites are shown for comparison.

RESULTS

(I) Quantitation of Cu(I) by XAS, Absorption, and EPR. To directly quantitate the amount of reduced copper in different samples of chicken Cp, we used copper K-edge XAS. Cu(I) exhibits an intense feature at ~8984 eV in the X-ray absorption spectrum, corresponding to an electric dipole-allowed 1s → 4p transition (*34*). The intensity of this feature relative to the normalized Cu K-edge can be used to quantitate the amount of Cu(I), and the shape can give information about the coordination number of a Cu(I) site. The XAS spectra for three different samples of chicken Cp are shown in Figure 1. Reduced chicken Cp (generated by addition of ~100-fold excess ascorbate) showed a complete loss of the absorption features at 330 and 610 nm and no EPR signal and, as expected, the XAS exhibits a large feature at 8983 eV. The resting sample also shows significant intensity at 8983 eV, indicating the presence of a substantial amount of reduced copper. The XAS spectrum of peroxide-oxidized Cp (Figure 1) does not show any residual intensity at 8983 eV, indicating that all of the copper is oxidized. In our previous studies (*23*), to quantitate the amount of reduced copper in resting and peroxide-oxidized human Cp a fully oxidized reference spectrum was constructed with the XAS of T1Hg derivative of laccase, in which the type 1 copper is replaced with mercury leaving just the oxidized trinuclear cluster (*10*), and the XAS of oxidized plastocyanin (*35*), a

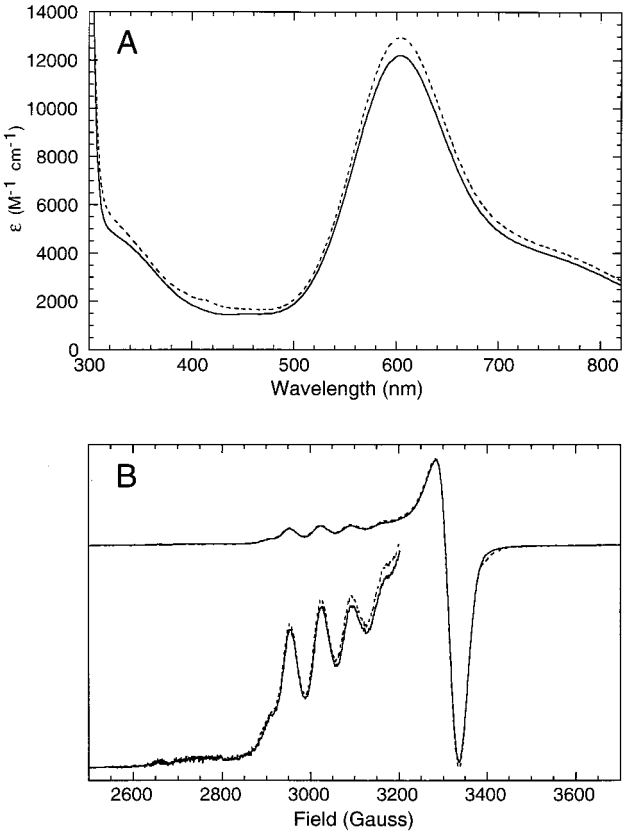

FIGURE 2: (A) Absorption spectra of resting (—) and peroxide-oxidized (- - -) chicken Cp. (B) EPR spectra of resting (—) and peroxide-oxidized (- - -) chicken Cp. Experimental conditions: temperature, 77 K; microwave frequency, 9.5085 GHz; microwave power, 20 mW; modulation amplitude, 16 G; modulation frequency, 100 kHz; time constant, 0.5 s.

Table 1: Quantitation of Reduced Copper, Paramagnetic Copper, and Absorption Intensities in Resting and Oxidized Chicken Cp

method	resting	oxidized
% reduced Cu by XAS	19.2 ± 5.0	0 ± 5.0
% paramagnetic Cu by EPR	48.7 ± 5.6	53.7 ± 5.3
% paramagnetic Cu by magnetic susceptibility	61.2 ± 7.0	72.5 ± 6.0
Molar absorptivity at 610 (M^{-1} cm^{-1})	12 270 ± 560	12 930 ± 810
Molar absorptivity at 330 (M^{-1} cm^{-1})	4600 ± 330	5110 ± 220

blue copper protein, weighted and normalized to one oxidized trinuclear cluster and three oxidized blue copper sites. This is shown for comparison in Figure 1. The XAS of peroxide-oxidized chicken Cp essentially overlays the constructed fully oxidized spectrum, confirming that in peroxide-oxidized chicken Cp all of the copper sites are oxidized. The intensity difference at 8983 eV between the model spectrum and fully reduced chicken Cp was used to quantitate the amount of reduced copper in the resting and peroxide-oxidized forms. From this, 0% ± 5.0% of the copper is reduced in peroxide-oxidized chicken Cp and 19.2% ± 5.0% is reduced in the resting enzyme (Table 1).

Representative absorption spectra of resting and peroxide-oxidized chicken Cp are shown in Figure 2A. The molar absorptivities of the 330 and 604 nm bands are 4600 ± 330 and 12 270 ± 560 M^{-1} cm^{-1}, respectively, in resting chicken Cp and 5110 ± 220 and 12 930 ± 810 M^{-1} cm^{-1} in peroxide-oxidized chicken Cp (Table 1). A small increase in intensity at about 412 nm also appears upon addition of peroxide, which appears to correlate with the appearance of a small amount of radical signal in the EPR spectrum of the peroxide-oxidized form (vide infra). Note that the ratio of the blue band relative to the 330 and 280 nm bands differs in peroxide-oxidized chicken Cp compared to human Cp. In oxidized chicken Cp, the 604/280 ratio is 0.064 and the 330/604 ratio is 0.40, while in oxidized human Cp, the 610/280 ratio is 0.045 and the 330/610 ratio is 0.52. From the change in band intensities upon oxidation with peroxide, one can obtain an upper limit on the amount of reduced T3 and T1 copper present in resting chicken Cp: ≤13% of the T3 copper and ≤7% of the T1 copper.

The X-band EPR spectra of resting and peroxide-oxidized chicken Cp at 77 K are shown in Figure 2B. As previously reported (*24*), the resting chicken Cp spectrum clearly shows the contribution from at least two different T1 copper sites, while the T2 copper signal normally present in all multi-copper oxidases is essentially absent, except for trace quantities of adventitious copper. A small amount of radical signal is also clearly present in the peroxide-oxidized sample, the intensity of which was variable and could be reduced by Centricon dialysis, passage of the protein through a G-25 column, or storage for about a day at 4 °C. The ratio of the low-field hyperfine lines from the different T1 copper centers in oxidized chicken Cp is about 1:3, considerably different from the 1:1.5 ratio seen in human Cp. The amount of paramagnetic copper in resting and peroxide-oxidized chicken Cp was determined by double integration of the X-band spectra relative to a copper standard. From this, the fraction of copper that is paramagnetic by EPR is 48.7% ± 5.6% in resting chicken Cp and 53.7% ± 5.3% in the peroxide-oxidized form (Table 1).

The XAS of resting chicken Cp indicates that 19.2% of the copper is reduced. Yet, the absorption data shows that no more than 13% of the T3 copper is reduced, and both the absorption and EPR data shows that about 5−7% of the T1 copper is reduced, accounting for substantially less than the amount of reduced copper seen by XAS. The fact that chicken Cp has oxidase activity provides firm evidence that it contains an intact T2/T3 trinuclear cluster; therefore, the reduced copper seen in the XAS of resting chicken Cp must be the T2 copper site. This explains why the EPR spectrum of resting chicken Cp lacks any features from a T2 copper site: this site is completely reduced. One would expect that, upon oxidation, a normal T2 copper EPR signal should appear; as seen in Figure 2B, this does not happen. A possible reason for this will be addressed below.

We can estimate the XAS K-edge spectrum of the reduced T2 copper site by subtraction of the fully oxidized model spectrum from the resting chicken Cp data (Figure 1, inset). The shape and intensity of the peak at 8983 eV can be used to probe the coordination number of a Cu(I) site. Two-coordinate Cu(I) has a peak maximum at 8983.9 ± 0.3 eV and an normalized amplitude of 1.08 ± 0.10, three-coordinate Cu(I) has a maximum at 8983.5 ± 0.4 eV and an amplitude of 0.63 ± 0.05, and four-coordinate Cu(I) has a maximum at 8985.5 ± 0.8 eV and an amplitude of 0.72 ± 0.06. The 8983 eV feature of the difference spectrum (Figure 1, insert) indicates that this Cu(I) is best described as intermediate between two- and three-coordinate (*21*), consistent with the crystal structure of the T2 copper center in reduced ascorbate oxidase.

Table 2: EPR Simulation Parameters of Chicken Cp at X- and Q-band Frequencies

	g value			*A* value (G)			Line width, X-band (G)			Line width, Q-band (G)		
Cu site	g_z	g_x	g_y	A_z	A_x	A_y	L_z	L_x	L_y	L_z	L_x	L_y
T1A	2.2600	2.0570	2.0385	64.0	9.5	9.5	30.0	32.5	32.5	52.5	46.0	39.0
T1B	2.2280	2.0570	2.0385	66.0	9.5	9.5	27.0	32.5	32.5	47.5	46.0	39.0
T1C	2.2205	2.0570	2.0385	74.0	9.5	9.5	27.0	32.5	32.5	47.5	46.0	39.0

Previous work indicated that chicken Cp contains 5 coppers per molecule and the copper stoichiometry was assigned as two T1 sites and a trinuclear cluster, which was assumed to be fully oxidized (*24*). The EPR spectrum quantitated to 50% of the total copper content, i.e., 2.5 paramagnetic copper sites per molecule. A nonintegral number of paramagnetic copper sites was explained by the presence of magnetic interactions between the T2 and T3 coppers leading to a broad, unresolved EPR signal that quantitated to less than 1 copper per molecule. We have now shown that in resting chicken Cp, the T1 copper sites are nearly fully oxidized and the T2 copper center is reduced, thus, the EPR spectrum should correspond to an integral number of copper sites. This would argue in favor of a copper stoichiometry of 3 T1 copper sites out of 6 total coppers per molecule, rather than 2 T1 sites out of 5 coppers per molecule, which is also consistent with the higher copper content reported herein (5.65 coppers per molecule). An unambiguous determination of the copper stoichiometry requires a precise molecule weight, which is not presently available.

The experimental X-band at 77 K and Q-band at 96 K EPR spectra of peroxide-oxidized chicken Cp are shown in Figure 3, panels A and B, respectively. These spectra were simulated in order to obtain a reasonable estimate of the spin Hamiltonian parameters for the different T1 copper sites. Adequate simulations were obtained with three T1 copper sites with equal double integrated intensities (i.e., equal amounts) but different parameters, as listed in Table 2. Severe spectral overlap from the three different copper sites precludes unambiguous determination all of the parameters in the $g_\perp$ region; however, the Q-band spectrum clearly shows a splitting in the $g_\perp$ region, indicating either the presence of at least two axial copper sites with significantly different $g_\perp$ values or at least one copper site that is significantly rhombic. While both possibilities gave reasonable simulations of the Q-band data, the latter better reproduced the shape of the $g_\perp$ region in the X-band spectrum; for simplicity, we have chosen to model all three copper sites as rhombic ($|g_x - g_y| = 0.0185$) with identical parameters in this region. One could also simulate the spectra with two T1 copper sites of equal amounts; however, to obtain the proper ratio of the T1 copper low-field hyperfine lines, the line width in the $g_\parallel$ region of one of the sites needed to be 1.75 times larger than the other. From a combination of the X-band and Q-band EPR data, the upper limit for the parallel hyperfine value of any of the copper sites is ~78 G, which is well below what is seen for the fungal laccases and Fet3 protein ($A_\parallel = 85-95$ G). The significance of this result will be discussed below.

(II) Spectroscopic and Magnetic Probes of the T2 Copper Center. SQUID magnetic susceptibility is a bulk technique for the quantitation of paramagnetic centers. Since it is not affected by relaxation properties, it can detect paramagnetic sites that may not appear in EPR. The slope of the magnetic susceptibility versus $1/T$ corresponds to the percent of the copper that is paramagnetic ($S = {}^1/_2$) multiplied by the theoretical Curie−Weiss constant for one Cu(II), which in this case was calculated with a g_{av} of 2.1106 derived from the *g* values determined by EPR simulation (vide infra). The Curie slope SQUID magnetic susceptibility data for resting and peroxide-oxidized chicken Cp are shown in Figure 4, along with theoretical lines calculated for two, three, four, and five paramagnetic copper sites out of six for comparison. The y-intercept corresponds to the diamagnetic correction and was set equal to zero. The error bars show the standard deviation in the slope of the experimental data. From the slope of the lines of best fit, 61.2% ± 7.0% of the copper in the resting enzyme is paramagnetic by SQUID magnetic susceptibility, while in the peroxide-oxidized chicken Cp, 72.5% ± 6.0% of the copper is paramagnetic (Table 1). There was no evidence for the population of a spin quartet state within the temperature range used in these experiments (5.25−115 K). These results differ from the amount of paramagnetic copper that was determined by EPR quanti-

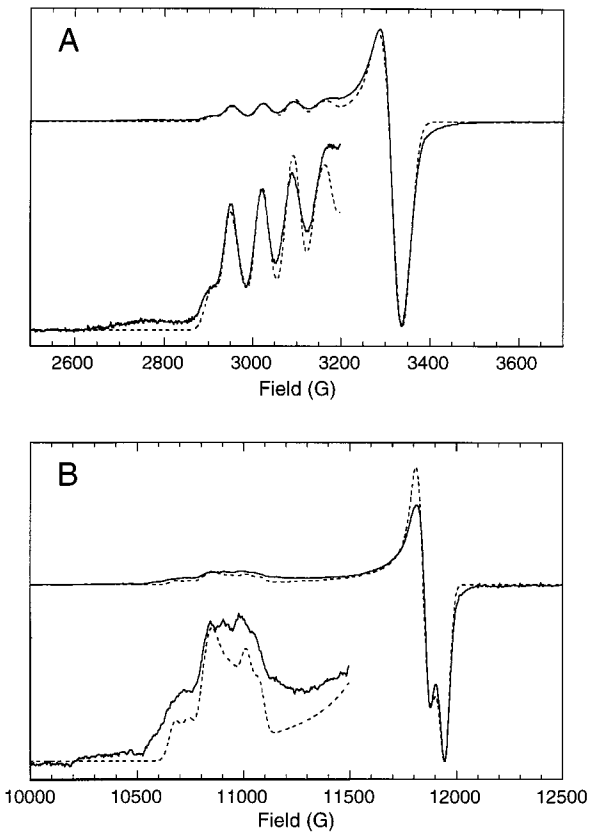

FIGURE 3: Experimental (—) and simulated (- - -) EPR spectra of peroxide-oxidized chicken Cp at (A) X-band (temperature, 77 K; microwave frequency, 9.508 GHz) and (B) Q-band (temperature, 98 K; microwave frequency, 34.08 GHz). Other experimental conditions: microwave power, 20 mW; modulation amplitude, 16 G; modulation frequency, 100 kHz; time constant, 0.5 s. Spin Hamiltonian parameters from the simulations are listed in Table 2.

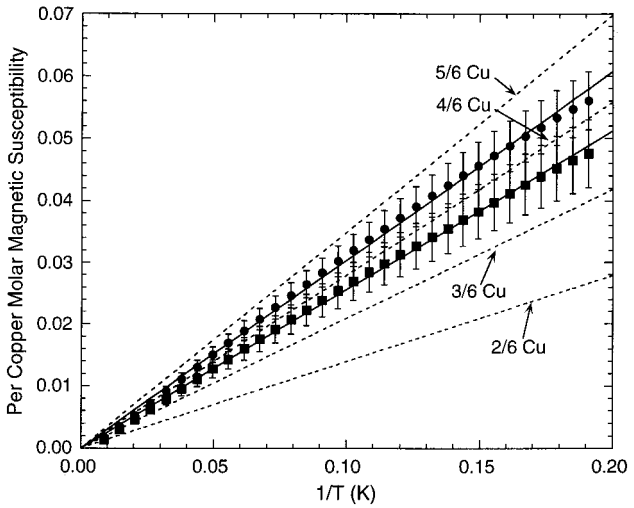

FIGURE 4: Per-copper molar magnetic susceptibility data for resting (■) and peroxide-oxidized (●) chicken Cp, along with the least-squares lines of best fit (—), error bars at 1 standard deviation unit, and theoretical lines for two, three, four, and five paramagnetic sites out of six total copper sites per molecule (- - -).

tation. Notably, there is a significant difference in the amount of paramagnetic copper detected by SQUID magnetic susceptibility between the resting and oxidized forms of chicken Cp: about 11% of the copper became paramagnetic upon oxidation. This contrasts with the results previously obtained on human Cp, in which there was good agreement between the amount of paramagnetic copper detected by EPR and magnetic susceptibility: both techniques showed that 12% of the copper became paramagnetic upon oxidation (*23*). This indicates that some fraction of copper in peroxide-oxidized chicken Cp is paramagnetic with $S = {}^1/_2$ but not observed in the EPR spectrum at 77 K.

From the above data, we have established the following: (1) the T2 copper site in chicken Cp is reduced in the resting form, (2) upon oxidation, it does not appear in the EPR spectrum at 77 K, and (3) it does contribute to the total amount of paramagnetic copper seen by magnetic susceptibility. We pursued EPR studies at liquid helium temperatures in order to see if the T2 copper signal could be observed only at lower temperatures due to a fast relaxation rate. Figure 5A shows the EPR spectra of resting and oxidized chicken Cp at a temperature of approximately 8 K and at 202 mW, 3.1 mW, and 5.0 μW (scaled by a factor of 5) of microwave power. The parallel hyperfine lines in the spectrum (field positions of ~2950 and 3020 G), which correspond to copper sites T1B and C from the EPR simulations above, saturate more easily than the low-field shoulder (~2910 G) and the troughs in the $g_{\|}$ region (~2980 G), which correspond to the T1A copper site, as also observed in the plot of the power saturation behavior (Figure 5C). Thus, at least two of the T1 copper sites have significantly different relaxation properties. Upon oxidation, all of the features of the T1 copper saturate slightly more easily than in the resting samples. Importantly, oxidation of the enzyme causes the appearance of a new, broad feature that grows in at higher power, which was not observed at 77 K. The difference spectra of the oxidized minus resting samples taken at each microwave power show the appearance of a broad, nearly isotropic signal centered at g ~2.07 (Figure 5B), which saturates much less readily at high microwave

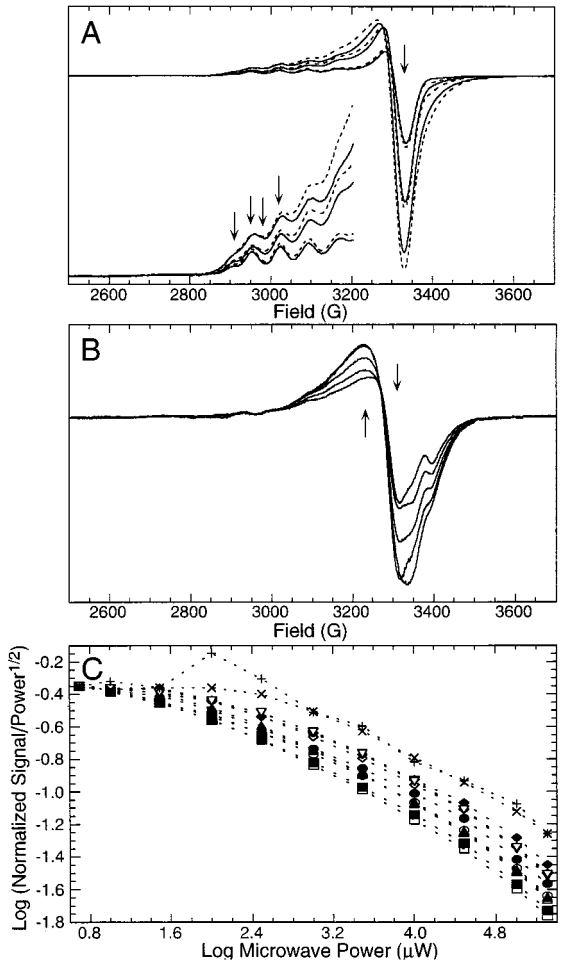

FIGURE 5: (A) EPR spectra of resting (—) and peroxide-oxidized (- - -) chicken Cp at three different microwave powers: 202 mW, 3.1 mW, and 5.0 μW (scaled by a factor of 5). Experimental conditions: temperature, ~8 K; microwave frequency, 9.5115 GHz; modulation amplitude, 20 G; modulation frequency, 100 kHz; time constant, 1.0 s. (B) Difference spectra of peroxide-oxidized minus resting chicken Cp at 201, 101, 31, 10.1, and 3.1 mW of microwave power. (C) Power saturation curves at ~8 K for the normalized EPR signal intensities in resting chicken Cp at the following field values: 2910 G (●), 2950 G (■), 2980 G (◆), 3020 G (▲), and 3330 G (▼). These field positions are denoted in panel A with arrows. The power saturation curves for peroxide-oxidized chicken Cp at the same field positions are indicated with the corresponding open symbols. Power saturation curves at ~8 K for the difference EPR spectra (normalized intensity) at 3230 G (×) and at 3310 G (+). These field positions are denoted in panel B with arrows.

power than the T1 copper sites (Figure 5C). To obtain the spin concentration of the new feature that appears in difference spectra, we double-integrated it at high power and back-extrapolated to low power from the shape of the microwave power saturation curve, yielding a rough estimate for the spin concentration of the new isotropic signal of 0.5 Cu.

Magnetic circular dichroism (MCD) spectroscopy provides another probe of paramagnetic metal sites which may be difficult to observe by EPR because of fast relaxation. Since only a negligible amount of T1 copper is oxidized upon addition of H_2O_2 to resting chicken Cp, the only significant new features to appear in the MCD spectrum should arise from the T2 copper. The MCD spectra of resting and oxidized chicken Cp at 5 K and 7 T are shown in Figure 6A. The MCD spectrum of resting chicken Cp exhibits the

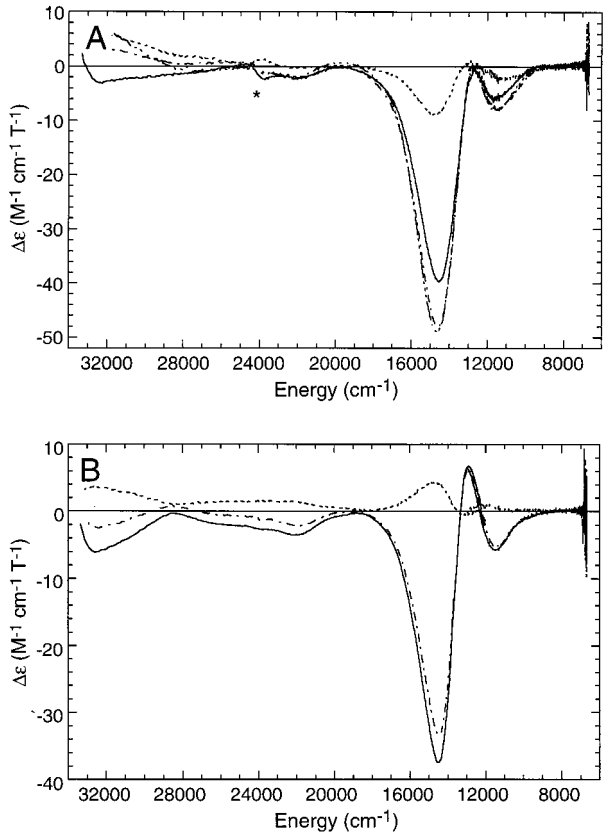

FIGURE 6: (A) MCD spectra of chicken Cp at 5 K and 7 T: resting (—), peroxide-oxidized (—•—), peroxide-oxidized with 20 equiv of fluoride (—•••—), and the difference spectrum of oxidized minus resting (- - -). An asterisk denotes a trace amount of a heme impurity. (B) MCD spectra of peroxide-oxidized human Cp without (—) and with (—•—) 20 equiv of fluoride, and the difference spectrum of with minus without fluoride (- - -) at 5 K and 7 T.

usual features associated with T1 copper, as seen previously in plastocyanin (*36*) and ascorbate oxidase (*37*): an intense negative band at 14 500 cm^{-1} ($d_{xz,yz} \rightarrow d_{x^2-y^2}$), a weaker negative band at 11 700 cm^{-1} ($d_{xy} \rightarrow d_{x^2-y^2}$), and a weak band at 22 100 cm^{-1} ($N_{His} \rightarrow$ Cu $d_{x^2-y^2}$). Upon oxidation, the features at 14 500 and 11 700 cm^{-1} become significantly more intense. The difference spectrum (Figure 6A) shows negative bands at 14 800 and 11 000 cm^{-1} which must be dominantly from T2 copper ligand field transitions. The energies and intensities of these new bands are very similar to the features previously assigned to T2 copper: the MCD spectrum of the T1 mercury derivative (T1Hg) of plant laccase exhibits ligand-field transitions at 18 400 (—), 14 100 (—), 12 100 (+), and 9400 cm^{-1} (+) (*38*, *39*), and ascorbate oxidase has a negative band at 13 700 cm^{-1} ($\Delta\epsilon \approx 7$ M^{-1} cm^{-1} T^{-1}), which was shown to be a T2 copper ligand field transition by use of the perturbation induced upon fluoride binding (vide infra) (*37*). Thus, the appearance of these new bands in the MCD spectrum is consistent with the appearance of a fully oxidized T2 copper site.

In fungal laccase, plant laccase, ascorbate oxidase, and human Cp it was previously found that two fluoride ions bind selectively to the T2 copper site, one with high affinity and one with low affinity (*40*—*42*). This is seen by EPR, in which fluoride-binding induces a superhyperfine splitting of about 50×10^{-4} cm^{-1} in the low-field hyperfine line of the T2 copper. This perturbation of the T2 copper site has also been seen by MCD in native (*9*) and T1Hg plant laccase (*38*) and in ascorbate oxidase (*37*), in which fluoride binding induces a dramatic decrease in the MCD intensities of the ligand-field transitions of the T2 site, particularly the one at about 14 000 cm^{-1}. We have now extended these results to human and chicken Cp. Peroxide-oxidized human Cp was incubated for at least 24 h at 4 °C with 20 equiv of fluoride. The EPR spectrum clearly showed the superhyperfine splitting of the T2 copper low-field hyperfine line due to fluoride binding, as previously reported (*40*, *42*). The MCD spectra at 5 K and 7 T of oxidized human Cp, oxidized human Cp plus 20 equiv of fluoride, and the difference spectrum are shown in Figure 6B. The spectrum of oxidized human Cp is again dominated by the spectral features of the two redox-active T1 copper sites, with ligand-field transitions at 14 500 (—), 12 900 (+), and 11 500 cm^{-1} (—) and a weak charge-transfer band at 22 000 cm^{-1} (—). Addition of fluoride perturbs the intense negative band at 14 500 cm^{-1} and the weaker, lower energy bands. These changes are seen in the difference spectrum, which shows the appearance of two positive features at 14 700 and 12 200 cm^{-1}, i.e., as previously observed in other multicopper oxidases, binding of fluoride decreases the intensity of the T2 copper MCD bands, causing these two negative bands to appear as positive features in the difference spectrum. Thus, the energy and intensity of the ligand field transitions of the oxidized T2 site in human Cp are similar to those in plant laccase and ascorbate oxidase. We then performed a parallel series of experiments on oxidized chicken Cp in order to determine if this unusual T2 site also bound fluoride. From both the X-band EPR at 77 K (data not shown) and the MCD spectrum at 5 K and 7 T (Figure 6A), incubation with 20 equiv of fluoride for at least 24 h at 4 °C has no effect. Up to 80 equiv of fluoride also has no effect on the EPR spectrum. These results indicate that the unusual T2 copper site in chicken Cp does not bind fluoride, in contrast to all of the other multicopper oxidases including human Cp.

(III) Thermodynamics and Kinetics of Electron Distribution in Chicken Cp. From a combination of XAS, absorption, and EPR, we have determined that in resting chicken Cp, the T2 copper is completely reduced, while only small amounts of the remaining copper sites are reduced. Overall, about 1.2 coppers out of 6 are reduced in the resting enzyme. To understand the origin of this redox distribution, we have performed reductive titrations of the peroxide-oxidized enzyme to probe the relative reduction potentials of the copper centers, and we have examined the reoxidation behavior of the copper sites.

Reductive titrations allow one to determine the equilibrium electron distribution in systems with multiple redox centers, such as the multicopper oxidases. In this method, *n* equiv of a sufficiently powerful reductant is added to a protein sample. After enough time is allowed to reach equilibrium, the fraction of each redox center that is reduced is quantitated on the basis of the change in an associated spectroscopic feature. This is repeated, varying the amount of reductant. The resulting curves are then fit to a series of coupled Nernst equations, which gives the relative potentials of the redox sites. In this case, Fe(II) was used as the reductant, since it rapidly reduces the copper in Cp. No precipitation of Fe(III) was observed, despite the use of pH 7.0 phosphate buffer. This is likely due to the low concentration of iron used and the binding of the Fe(III) by the protein. The

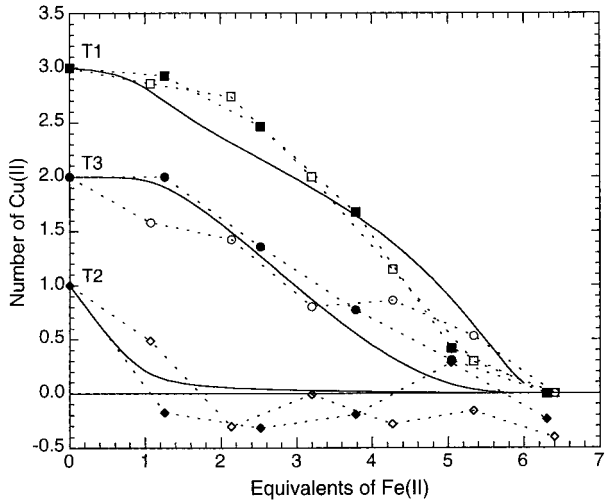

FIGURE 7: Anaerobic reductive titration of peroxide-oxidized chicken Cp with Fe(II) as the reductant. The number of oxidized T1 coppers (■) was quantitated from the absorption intensity at 604 nm; the number of oxidized T3 copper (●) was quantitated by using the absorption intensity at 330 or 360 nm (see text for details); the number of oxidized T2 coppers (◆) was quantitated based upon the amount of reductant and the amount of reduced T1 and T3 copper. Open symbols correspond to a second complete set of titration data using a different batch of protein. Solid lines were calculated from a set of coupled Nernst equations incorporating the differences in reduction potentials among the different copper sites.

presence of soluble Fe(III) species was evident from the presence of an Fe(III) charge-transfer band at 310 nm and a $g = 4.3$ signal in the EPR spectrum. Tight binding of Fe(III) has previously been observed in human Cp (*43*). The number of oxidized T1 copper sites (assuming three total) was quantitated from the difference in the intensity of the 604 nm absorption band relative to that in the fully oxidized and fully reduced forms. In principle, the number of T3 coppers could be quantitated from the change in intensity of the 330 nm absorption band; however, the Fe(III) charge-transfer band interfered with direct measurement of the 330 nm band. Two strategies were adopted to quantitate the amount of reduced T3 copper: either the intensity of the low-energy tail of the T3 copper band was measured (360 nm), or after reduction, the sample was exposed to air. Since the 330 nm band completely returns rapidly upon exposure to dioxygen (vide infra), the difference in intensity between the reduced and reoxidized samples at 330 or 360 nm yields the fraction of oxidized T3 copper. These two methods gave similar results. The fraction of reduced T2 copper was calculated from the difference between the amount of reductant added and the amount of T1 and T3 copper reduced. Addition of 7 equiv of Fe(II) yielded an absorption spectrum identical to that of the sample reduced with only 6 equiv of Fe(II), including the intensity of the Fe(III) charge-transfer bands. This confirms (1) the potential of the Fe(II)/(III) couple is much lower than that of any of the copper sites and (2) all of the copper sites were reduced upon the addition of 6 equiv of Fe(II), including copper sites that might lack intense absorption bands. The results of two separate reductive titration experiments (closed and open symbols) on peroxide-oxidized chicken Cp are shown in Figure 7. From these data, it is clear that little of the T1 (squares) and T3 copper (circles) is reduced upon addition of the first 1−2 equiv of reductant. This implies that the T2 copper (diamonds) is thermodynamically the easiest to reduce, i.e., it has the highest reduction potential. Quantitation of the relative redox potentials of the copper sites was obtained from the fits to the data (solid lines, Figure 7). In these simulations, a number of assumptions are made: (1) the T3 site behaves strictly as a two-electron oxidant, and (2) the potential of any one copper site is not affected by the redox state of any of the other copper sites nor by the binding of Fe(II) or Fe(III) to the protein. We obtain the best fit to the data with the potential of the T2 site about 85 mV higher than the other sites. All of the other sites appear to have similar potentials; the best fit has the T3 site with a potential about 12 mV higher than the T1 sites. The T1 sites were all fit with the same potential. While this is an oversimplification, it appears from fits to the data that the T1 copper centers do not have dramatically different potentials (within 50 mV).

We examined the reoxidation by dioxygen of chicken Cp reduced with 6 equiv of Fe(II) and found results consistent with those previously reported with ascorbate as the reductant (*24*): the 330 nm band and approximately 67% of the blue band returns quickly (less than 30 s), and although the remaining 33% returns more slowly, all of it reappears. This provides a basis for understanding the redox distribution observed in resting chicken Cp. Upon reoxidation by dioxygen, four of the copper sites are oxidized, presumably one T1 copper and the trinuclear copper cluster from analogy to laccase. Reestablishment of redox equilibrium among the copper sites would lead to rereduction of the T2 copper site and therefore one reducing equiv distributed among the three T1 copper sites, corresponding to what is initially observed by absorption spectroscopy. Over time, the remaining T1 copper is oxidized by outer-sphere oxidation with dioxygen, which is more rapid than that seen in human Cp. This would yield the redox distribution found in the resting form of the enzyme.

DISCUSSION

Our results provide new insight into the copper and redox stoichiometry of chicken Cp, which shows a number of key differences relative to human Cp. XAS, absorption, and EPR show that all of the copper sites are oxidized in peroxide-oxidized chicken Cp and that the T2 copper center is reduced in the resting enzyme. In human Cp, one of the T1 copper sites (likely the one in domain two, which lacks an axial methionine ligand) is reduced and cannot be oxidized due at least in part to a high redox potential (*23*), and one additional reducing equiv in the resting enzyme is distributed mostly on the two redox-active T1 copper sites. In the initial report on the isolation of chicken Cp, the enzyme was proposed to contain five copper sites; however, now that the T2 copper site is found to be reduced in the resting enzyme, an alternate interpretation yields a copper content of six copper sites per molecule: three T1 sites and a T2/T3 trinuclear cluster. This proposal is in keeping with the copper content of human Cp, with the crucial difference that in chicken Cp all of the T1 copper is redox-active. Indeed, the reductive titration experiments indicate that all of the T1 copper sites in chicken Cp have similar potentials. Insight into the reason for this difference is obtained from examination of the EPR simulation parameters. The best simulation (assuming six coppers per molecule) was obtained with three

T1 copper sites with parallel hyperfine values of 64, 66, and 74 G. "Classical" blue copper sites with Cys-His-His-Met ligation (plastocyanin, the T1 copper site in ascorbate oxidase, and the two redox-active T1 copper sites in human Cp) all have parallel hyperfine values of 35−76 G (*1*, *44*), while known redox-active three-coordinate T1 copper sites in which the axial methionine ligand has been replaced in the amino acid sequence with either a leucine or a phenylalanine (the fungal laccases and FET3) have parallel hyperfine values of 85−95 G (*1*, *3*, *4*). A copper site in chicken Cp with such a large parallel hyperfine value can be ruled out by a combination of the X-band and Q-band EPR data. The permanently reduced T1 site (T1PR) in domain 2 in human Cp is three-coordinate and lacks an axial methionine. Thus, in chicken Cp either copper is absent from this site or this site contains a redox-active T1 copper with a methionine or other axial ligand. The lack of an axial methionine ligand correlates with a higher redox potential in T1 copper sites, as has been seen experimentally in mutagenesis experiments on azurin (*45*) and in many of the fungal laccases (*46*, *47*). Other factors, such as the orientation of amide dipoles and solvent accessibility, could also contribute to the difference in redox potential between the T1 site in domain two in human Cp and an analogous site in chicken Cp.

Although oxidation of chicken Cp does not lead to the appearance of T2 copper EPR features at 77 K, the fact that the enzyme is active, along with the appearance of an additional paramagnetic species by SQUID magnetic susceptibility and MCD, provides direct evidence for a paramagnetic T2 copper center. The MCD of the oxidized minus resting difference spectrum shows negative bands at 14 800 and 11 000 cm^{-1}, which we have assigned as ligand field transitions of the T2 copper, similar to other multicopper oxidases. However, this copper center displays two major differences: a broad, featureless, nearly isotropic EPR feature centered at $g \approx 2.07$ at ~8 K that is harder to saturate than the T1 copper sites, and no evidence of fluoride binding to this site by either EPR or MCD. The existence of a fast-relaxing, featureless, nearly isotropic EPR signal can be accounted for by coupling of the T2 copper with the T3 copper pair to yield a net $S = {}^1/_2$ ground state, as was originally postulated by Calabrese et al. (*24*). A model for understanding the ground state electronic structure and magnetic properties of an exchange-coupled copper trimer in terms of a set of three exchange coupling constants has been previously presented (*38*). From this, it is possible for an $S = {}^1/_2$ copper trimer to have a **g** tensor with little anisotropy and to have no discernible hyperfine splitting, in contrast to the usual case for an isolated Cu(II) ion. Likewise, the greater relaxation rate of such a species may arise from the presence of an Orbach mechanism for relaxation due to the presence of an additional $S = {}^1/_2$ excited state at low energy. Exchange coupling between the T2 copper and at least one of the T3 coppers in chicken Cp would require the presence of an additional bridging ligand between these copper sites. Note that a broad, featureless, fast-relaxing EPR signal is observed in the native intermediate of laccase (*48*). This signal has also been assigned as arising from an oxidized copper trinuclear cluster with an additional ligand bridging between the T2 and T3 copper sites. An additional bridging ligand would also provide a possible explanation for the lack of fluoride binding.

In resting chicken Cp, 1.2 out of the 6 coppers are reduced: all of the T2 copper is reduced, and most of the remaining 0.2 reducing equivalent is distributed on the T3 site. In contrast, resting human Cp contains one extra reducing equiv in addition to the T1PR site, which is distributed among the T1, T2, and T3 sites in the ratio of roughly 0.5:0.3:0.2. Two factors contribute to this difference: the relative redox potentials of the copper sites and the rate at which the T1 sites are reoxidized by dioxygen in an outer-sphere process. In the case of the T1 copper sites in human Cp, the outer-sphere oxidation rate appears to be slow, since upon reduction of the fully oxidized form and reoxidation with dioxygen only about 50% of the blue band reappears; the rest does not reoxidize for many hours (*26*, *27*).[3] Therefore, the redox distribution roughly correlates with the relative redox potentials. In chicken Cp, we have measured the relative potentials of the copper sites and find that, indeed, the potential of the T2 site is higher than that of the other sites, in keeping with the fact that it is reduced in the resting form. The difference in the relative redox potentials of the copper sites in human vs chicken Cp could reflect the different geometric and electronic structure of the trinuclear cluster due to coupling between the T2 and T3 copper sites in chicken Cp. However, chicken Cp differs from human in that all of the T1 upper is oxidized in the resting form and all of it reappears upon reduction and reoxidation, thus implying a difference in the rate of outer-sphere oxidation.

In our previous work, we proposed that the T1 site in domain two of human Cp is not catalytically relevant because it cannot be oxidized due to a high reduction potential. One hypothesis for the existence of such a site is that it is an evolutionary vestige, since the multicopper oxidases are believed to have arisen from the duplication of an ancestral blue copper gene followed by loss of the blue copper site from some domains, addition of the trinuclear cluster, and (for the other multicopper oxidases) loss of whole domains (*51*−*54*). Previously published data on Cp isolated from cows (*55*, *56*), sheep (*57*, *58*), and dolphins (*59*) are consistent with the copper stoichiometry of human Cp; i.e., they also contain a T1PR site. Spectroscopic data of Cp isolated from turtles (*60*) and geese (*61*) more closely resembles that of chicken Cp; these likely also contain three redox-active T1 sites. Thus, some of the properties of a functional T1 copper site have been retained in the nonmammalian Cps (i.e., physiologically accessible redox potential) but lost in the mammalian Cps.

In summary, in chicken Cp all of the copper is redox-active and all of the T1 copper sites are four-coordinate, in contrast to human Cp. The T2 copper site is present and is paramagnetic in the oxidized form of the enzyme but can only be observed in the EPR spectrum at liquid helium temperature because it is fast-relaxing and broad, which likely reflects the presence of coupling with the T3 copper pair (*24*). It can be directly observed in the MCD spectrum, which is not affected by relaxation properties. The spectroscopic

[3] Note that when starting from the native form, in which much of the T1 copper is reduced, reduction and reoxidation again leads to much of the T1 copper remaining reduced (*49*). Also, the addition of chloride to human Cp alters the kinetics of reoxidation (*50*); such an effect has not been explored in chicken Cp.

differences between human and chicken Cp in their resting forms stem from differences in the relative redox potentials of the copper sites and possibly from differences in the rate of outer-sphere oxidation of the T1 sites by dioxygen. The differences in the properties of the copper sites in human vs chicken Cp seem to correlate with mammalian vs nonmammalian Cps, thus lending credence to the hypothesis of the evolutionary origin of the six-domain structure and multiple T1 copper sites in Cp (*50*−*53*).

REFERENCES

1. Solomon, E. I., Sundaram, U. M., and Machonkin, T. E. (1996) *Chem. Rev. 96*, 2563−2605.
2. Askwith, C., Eide, D., Van Ho, A., Bernard, P. S., Li, L., Davis-Kaplan, S., Sipe, D. M., and Kaplan, J. (1994) *Cell 76*, 403−410.
3. Kosman, D. J., Hassett, R., Yuan, D. S., and McCracken, J. (1998) *J. Am. Chem. Soc. 120*, 4037−4038.
4. Hassett, R. F., Yuan, D. S., and Kosman, D. J. (1998) *J. Biol. Chem. 273*, 23274−23282.
5. Barry, C. E., Nayar, P. G., and Begley, T. P. (1989) *Biochemistry 28*, 6323−6333.
6. Freeman, J. C., Nayar, P. G., Begley, T. P., and Villafranca, J. J. (1993) *Biochemistry 32*, 4826−4830.
7. Hsieh, C.-J., and Jones, G. H. (1995) *J. Bacteriol. 177*, 5740−5747.
8. Allendorf, M. D., Spira, D. J., and Solomon, E. I. (1985) *Proc. Natl. Acad. Sci. U.S.A. 82*, 3063−3067.
9. Spira-Solomon, D. J., Allendorf, M. D., and Solomon, E. I. (1986) *J. Am. Chem. Soc. 108*, 5318−5328.
10. Cole, J. L., Tan, G. O., Yang, E. K., Hodgson, K. O., and Solomon, E. I. (1990) *J. Am. Chem. Soc. 112*, 2243−2249.
11. Messerschmidt, A., Ladenstein, R., Huber, R., Bolognesi, M., Avigliano, L., Petruzzelli, R., Rossi, A., and Finazzi-Agro, A. (1992) *J. Mol. Biol. 224*, 179−205.
12. Messerschmidt, A., Luecke, H., and Huber, R. (1993) *J. Mol. Biol. 230*, 997−1014.
13. Ducros, V., Brzozowski, A. M., Wilson, K. S., Brown, S. H., Østergaard, P., Schneider, P., Yaver, D. S., Pedersen, A. H., and Davis, G. J. (1998) *Nat. Struct. Biol. 5*, 310−316.
14. Huber, C. T., and Frieden, E. (1970) *J. Biol. Chem. 245*, 3973−3978.
15. Zaitseva, I., Zaitsev, V., Card, G., Moshov, K., Bax, B., Ralph, A., and Lindley, P. (1996) *J. Biol. Inorg. Chem. 1*, 15−23.
16. Kasper, C. B., Deutsch, H. F., and Beinert, H. (1963) *J. Biol. Chem. 238*, 2338−2342.
17. Andréasson, L.-E., and Vänngård, T. (1970) *Biochim. Biophys. Acta 200*, 247−257.
18. Deinum, J., and Vänngård, T. (1973) *Biochim. Biophys. Acta 310*, 321−330.
19. Calabrese, L., Malatesta, F., and Barra, D. (1981) *Biochem. J. 199*, 667−673.
20. Calabrese, L., Mateescu, M. A., Carbonaro, M., and Mondovi, B. (1988) *Biochem. Int. 16*, 199−208.
21. Musci, G., Bonaccorsi di Patti, M. C., and Calabrese, L. (1993) *Arch. Biochem. Biophys. 306*, 111−118.
22. Calabrese, L., Carbonaro, M., and Musci, G. (1989) *J. Biol. Chem. 264*, 6183−6187.
23. Machonkin, T. E., Zhang, H. H., Hedman, B., Hodgson, K. O., and Solomon, E. I. (1998) *Biochemistry 37*, 9570−9578.
24. Calabrese, L., Carbonaro, M., and Musci, G. (1988) *J. Biol. Chem. 263*, 6480−6483.
25. Magdoff-Fairchild, B., Low, F. M., and Low, B. W. (1969) *J. Biol. Chem. 244*, 3497−3499.
26. Carrico, R. J., Malmström, B. G., and Vänngård, T. (1971) *Eur. J. Biochem. 22*, 127−133.
27. De Ley, M., and Osaki, S. (1975) *Biochem. J. 151*, 561−566.
28. Goa, J. (1957) *Scand. J. Clin. Lab. Invest. 5*, 218−222.
29. Felsenfeld, G. (1960) *Arch. Biochem. Biophys. 87*, 247−251.
30. Carithers, R. P., and Palmer, G. (1981) *J. Biol. Chem. 256*, 7967−7976.
31. Stern, E. A., and Heald, S. M. (1979) *Rev. Sci. Instrum. 50*, 1579−1582.
32. Lytle, F. W., Greegor, R. B., Sandstrom, D. R., Marques, E. C., Wong, T., Spiro, C. L., Huffman, G. P., and Huggins, R. E. (1984) *Nucl. Instrum. Methods 226*, 542−548.
33. Reinhammar, B. R. M., and Vänngård, T. I. (1971) *Eur. J. Biochem. 18*, 463−468.
34. Kau, L.-S., Spira-Solomon, D. J., Penner-Hahn, J. E., Hodgson, K. O., and Solomon, E. I. (1987) *J. Am. Chem. Soc. 109*, 6433−6442.
35. Penner-Hahn, J. E., Murata, M., Hodgson, K. O., and Freeman, H. C. (1989) *Inorg. Chem. 28*, 1826−1832.
36. Gewirth, A. A., and Solomon, E. I. (1988) *J. Am. Chem. Soc. 110*, 3811−3819.
37. Cole, J. L., Avigliano, L., Morpurgo, L., and Solomon, E. I. (1991) *J. Am. Chem. Soc. 113*, 9080−9089.
38. Cole, J. L., Clark, P. A., and Solomon, E. I. (1990) *J. Am. Chem. Soc. 112*, 9534−9548.
39. Sundaram, U. M., Zhang, H. H., Hedman, B., Hodgson, K. O., and Solomon, E. I. (1997) *J. Am. Chem. Soc. 119*, 12525−12540.
40. Brändén, R., Malmström, B. G., and Vänngård, T. (1973) *Eur. J. Biochem. 36*, 195−200.
41. Aikazyan, V. T., and Nalbandyan, R. M. (1977) *Biokhimiya 42*, 2027−2034.
42. Dawson, J. H., Dooley, D. M., and Gray, H. B. (1978) *Proc. Natl. Acad. Sci. U.S.A. 75*, 4078−4081.
43. Lindley, P. F., Card, G., Zaitseva, I., Zaitsev, V., Reinhammar, B., Selin-Lindgren, E., and Yoshida, K. (1997) *J. Biol. Inorg. Chem. 2*, 454−463.
44. Solomon, E. I., Baldwin, M. J., and Lowery, M. D. (1992) *Chem. Rev. 92*, 521−542.
45. Pascher, T., Karlsson, B. G., Nordling, M., Malmström, B. G., and Vänngård, T. (1993) *Eur. J. Biochem. 212*, 289−296.
46. Malmström, B. G., Reinhammar, B., and Vänngård, T. (1968) *Biochim. Biophys. Acta 156*, 67−76.
47. Xu, F., Shin, W., Brown, S. H., Wahleithner, J., Sundaram, U. M., and Solomon, E. I. (1996) *Biochim. Biophys. Acta 1292*, 303−311.
48. Aasa, R., Brändén, R., Deinum, J., Malmström, B. G., Reinhammar, B., and Vänngård, T. (1976) *FEBS Lett. 61*, 115−118.
49. Musci, G., Bonaccorsi di Patti, M. C., and Calabrese, L. (1993) *Arch. Biochem. Biophys. 306*, 111−118.
50. Musci, G., Bonaccorsi di Patti, M. C., and Calabrese, L. (1995) *J. Protein Chem. 14*, 611−619.
51. Ortel, T. L., Takashi, N., and Putnam, F. W. (1984) *Proc. Natl. Acad. Sci. U.S.A. 81*, 4761−4765.
52. Messerschmidt, A., and Huber, R. (1990) *Eur. J. Biochem. 187*, 341−352.
53. Ryden, L. G., and Hunt, L. T. (1993) *J. Mol. Evol. 36*, 41−66.
54. Murphy, M. E. P., Lindley, P. F., and Adman, E. T. (1997) *Protein Sci. 6*, 761−770.
55. Calabrese, L., Malatesta, F., and Barra, D. (1981) *Biochem. J. 199*, 667−673.
56. Sakurai, T., and Nakahara, A. (1986) *Inorg. Chim. Acta 123*, 217−220.
57. Calabrese, L., Capuozzo, E., Galtieri, A., and Bellocco, E. (1983) *Mol. Cell. Biochem. 51*, 129−132.
58. Calabrese, L., and Carbonaro, M. (1986) *Biochem. J. 238*, 291−295.
59. Bonaccorsi di Patti, M. C., Galtieri, A., Giartosio, A., Musci, G., and Calabrese, L. (1992) *Comp. Biochem. Physiol. 103B*, 183−188.
60. Musci, G., Carbonaro, M., Adriani, A., Lania, A., Galtieri, A., and Calabrese, L. (1990) *Arch. Biochem. Biophys. 279*, 8−13.
61. Hilewicz-Grabska, M., Zgirski, A., Krjewski, T., and Planka, A. (1988) *Arch. Biochem. Biophys. 260*, 18−27.

BI990280Z